ISA Transactions 85 (2019) 60–70

Contents lists available at ScienceDirect

ISA Transactions

journal homepage: www.elsevier.com/locate/isatrans

Research article

Static output feedback stabilization of networked control systems with a parallel-triggered scheme☆

Zhiying Wu [a,b], Yan Wang [a], Junlin Xiong [a,*], Min Xie [b]

[a] Department of Automation, University of Science and Technology of China, Hefei 230026, China
[b] Department of Systems Engineering and Engineering Management, City University of Hong Kong, Kowloon, Hong Kong

HIGHLIGHTS

- A new parallel-triggered scheme is proposed for networked control systems.
- The new scheme can reduce transmission rate while maintaining the system stability.
- A co-design algorithm is developed to minimize transmission rate.

ARTICLE INFO

Article history:
Received 30 March 2018
Received in revised form 1 September 2018
Accepted 28 September 2018
Available online 12 October 2018

Keywords:
Co-design
Event-triggered scheme
Networked control systems
Parallel-triggered scheme
Static output feedback

ABSTRACT

This paper investigates the parallel-triggered static output feedback stabilization problem for linear networked control systems. A new parallel-triggered scheme is proposed by using both the relative error and the absolute error information. The scheme can reduce transmission rate while maintaining the global asymptotical stability. The linear parallel-triggered networked control system is modeled as a time-delay system. By employing Lyapunov stability theory, sufficient conditions are established for the closed-loop system to be globally asymptotically stable in terms of linear matrix inequalities. Moreover, a co-design algorithm is developed to obtain both the optimal trigger parameters and the output feedback controller gain in the sense that the transmission rate is minimized. Finally, two examples are given to illustrate the advantages of the proposed scheme.

© 2018 ISA. Published by Elsevier Ltd. All rights reserved.

1. Introduction

Networked control systems (NCSs) are a class of distributed systems utilizing a communication network to exchange information among system components (sensors, actuators and controllers) [1]. NCSs have been widely applied in smart grids [2] and manufacture plants [3,4], and fruitful theoretical results of NCSs have been derived in [5–7]. Most of these results are established under a time-triggered scheme. In time-triggered NCSs, the sampled data are transmitted under a constant rate. However, the time-triggered scheme usually leads to over-utilization of the communication bandwidth. In practice, the communication bandwidth is limited. To reduce the consumption of communication resources, event-triggered schemes (ETSs) are adopted for NCSs [8–10].

In event-triggered NCSs, the control signals are updated only when event-triggered conditions are satisfied [8,10]. Recently, the event-triggered control problems have attracted substantial attention, and various ETSs are proposed to reduce the number of transmitted signals [10–21]. These ETSs can be classified into three types in terms of triggered conditions: the relative, the absolute and the mixed ETSs. In the relative ETSs, the event generators utilize the relative error information. Specifically, a continuous relative ETS is proposed in [11]. Based on the continuous relative ETS, the output feedback control problem for distributed NCSs is addressed in [12]. The continuous relative ETS may lead to Zeno behavior [22]. To avoid Zeno behavior, a periodic relative ETS for linear NCSs is proposed in [10]. Based on the periodic relative ETS, the static output feedback stabilization problem of linear NCSs is investigated in [13]. In the absolute ETSs, the event generators use the absolute error information. To be specific, an absolute ETS is proposed in [14] based on a constant threshold. To reduce the transmission rate during the transient state, an absolute ETS is firstly proposed in [15] by using an exponentially decreasing threshold function. Based on the absolute ETS in [15], an absolute ETS is presented in [16] by introducing a tuning parameter and a weighting matrix. Under the absolute ETS, the observer-based output feedback control problem of linear NCSs is discussed in

☆ This work was supported by National Natural Science Foundation of China under Grant 61773357 and 71532008.

* Corresponding author.
E-mail addresses: wzy100@mail.ustc.edu.cn (Z. Wu), wangyany@mail.ustc.edu.cn (Y. Wang), xiong77@ustc.edu.cn (J. Xiong), minxie@cityu.edu.hk (M. Xie).

https://doi.org/10.1016/j.isatra.2018.09.027
0019-0578/© 2018 ISA. Published by Elsevier Ltd. All rights reserved.

[16]. The relative and the absolute ETSs provide an efficient way of reducing the number of signal transmissions. In the mixed ETSs, the triggers use both the relative error and the absolute error information to further reduce the amount of transmitted signals. Specifically, a mixed ETS is proposed in [17] by using an additional threshold function. The advantage of using both the relative error and the absolute error information is verified in [17,18]. However, it is observed that stricter triggered conditions may not always result in the reduction in the amount of data transmissions (see Fig. 5 in this paper). The reason is that using the strict triggered condition, the system performance is deteriorated at the beginning of system operation, and hence more signals need to be transmitted in the following time. Motivated by the above discussion, it is important to develop an alternative scheme to further reduce transmission rate.

A new parallel-triggered scheme (PTS) is proposed in this paper by using both the relative error and the absolute error information. In our PTS, the sampled data are transmitted to the controller only when the following two conditions hold. One is the relative event-triggered condition presented in [10], and the other is the absolute event-triggered condition proposed in [16]. Compared with the event-triggered conditions in [10–21], the proposed parallel-triggered condition consists of two sub-conditions. Compared to the continuous triggered schemes in [11,12,14,18,19,23], our PTS only needs a supervision of the sampled data at discrete time instants and hence avoids the extra hardware requirements. The trigger under the PTS in [23] uses the absolute state information, whereas the trigger under our PTS uses the absolute error information.

Based on the proposed PTS, the static output feedback stabilization problem of linear NCSs is investigated in this paper. The linear parallel-triggered NCS is represented by a time-delay system. The following difficulties are involved: (1) for stability analysis, the system under the proposed PTS stays either in the relative ETS or in the absolute ETS. Moreover, the dwell time of the system staying in the relative ETS and the absolute ETS may be unknown. However, the methods in [10,13,15,16] are applicable to the systems staying in single ETSs only. (2) for co-design, it is desirable to obtain both the optimal trigger parameters and the output feedback controller gain. However, the methods in [10,13,15–17] find the feasible solutions only. The co-design method in [21] seeks for the optimal trigger parameters and the state feedback controller gain only. Besides, the trigger parameters in this paper are more flexible than those in [10,13,15–17,21]. To overcome the difficulties, we develop a new Lyapunov function for the system under the two ETSs. By employing Lyapunov stability theory, sufficient conditions are derived for global asymptotical stability by means of linear matrix inequalities (LMIs). Furthermore, a co-design algorithm is proposed to obtain both the optimal trigger parameters and the output feedback controller gain to minimize transmission rate. Finally, the effectiveness of the proposed PTS is illustrated by two examples.

The main contributions of this paper are summarized as follows: Firstly, a new PTS is proposed for NCSs. The examples show that the proposed scheme can further reduce the amount of transmitted signals compared to the existing schemes. Secondly, based on the new Lyapunov function, new sufficient conditions are derived for global asymptotical stability. Besides, new sufficient conditions are established for the output feedback controller design by using a new lemma. Thirdly, a co-design algorithm is proposed to obtain both the optimal trigger parameters and the output feedback controller gain.

Notation: $X > 0$ ($X < 0$) is a symmetric and positive (negative) definite matrix. $\mathbb{R}^n$ is the n-dimensional Euclidean space, and $\mathbb{R}^{m\times n}$ is the set of all $m \times n$ real matrices. The superscripts "T" and "-1" denote the matrix transposition and the matrix inverse, respectively, and $(X + X^T)$ is denoted by $\mathrm{He}(X)$. I_m and $0_{m\times n}$ represent the $m \times m$ identity matrix and the $m \times n$ zero matrix, respectively. $\mathbb{N}$ and $\mathbb{N}_{>0}$ denote the sets of nonnegative and positive integers, respectively. The symbol "$\star$" denotes the matrix entry implied by symmetry.

2. Problem statement

Consider the following linear continuous-time system:

$$\begin{cases}\dot{x}(t) = Ax(t) + Bu(t),\\ y(t) = Cx(t),\end{cases} \tag{1}$$

where $x(t) \in \mathbb{R}^n$ is the system state, $u(t) \in \mathbb{R}^m$ is the control input, $y(t) \in \mathbb{R}^p$ is the system output, and A, B and C are system matrices with appropriate dimensions.

The framework of a linear parallel-triggered NCS is demonstrated in Fig. 1. The system outputs are sampled periodically. The releasing signals are determined by the PTS, and are sent out to the controller through the network with communication delay.

By using both the relative error and the absolute error information, a new parallel-triggered condition is proposed as follows:

$$\begin{cases}e^T(j_kh)\Phi e(j_kh) \geq \delta y^T(j_kh)\Phi y(j_kh),\\ e^T(j_kh)\Phi e(j_kh) \geq \gamma(j_kh),\end{cases} \tag{2}$$

where $\delta \in [0, 1)$ is a constant, $\Phi > 0$ is a weighting matrix, $\gamma(t) = c\varepsilon^{-\alpha t}$ is the given threshold function with the parameters $c \geq 0$, $\varepsilon > 1$, and $\alpha > 0$. In addition, $e(j_kh) \triangleq y(t_kh) - y(j_kh)$, h denotes the sampling period, t_kh, $t_k \in \mathbb{N}$, is the latest triggered time, and $j_kh = t_kh + dh$, $d \in \mathbb{N}_{>0}$, is the present sampled time. Assume that $t_0 = 0$.

When the two inequalities in (2) are satisfied, the current sampled data are transmitted to the controller. Consider the triggered time sequence $\{t_0h, t_1h, t_2h, \dots\}$. It follows from (2) that the triggered time under the PTS is determined by

$$t_{k+1}h = t_kh + \min_{d\in\mathbb{N}_{>0}}\{dh|e^T(j_kh)\Phi e(j_kh) \geq \max\{\delta y^T(j_kh)\Phi y(j_kh), \gamma(j_kh)\}\}. \tag{3}$$

When $\gamma(j_kh) \leq \delta y^T(j_kh)\Phi y(j_kh)$, the system is under the relative ETS, otherwise the system is under the absolute ETS. The two sub-conditions of PTS (3) work together, then PTS (3) can provide longer inter-event intervals than the ETSs in [9,10,15,16] (see Theorem 3).

Remark 1. The proposed PTS (3) is characterized by the parameters $\delta, \Phi, c, \varepsilon$ and α, which affect the number of transmitted signals. Moreover, PTS (3) is a generalization of the relative ETSs [9,10] and the absolute ETSs [15,16]. Specifically, if $0 < \delta < 1$ and $c = 0$, then PTS (3) is reduced to the relative ETS in [9,10]. If $\delta = 0$ and $c > 0$, then PTS (3) is simplified as the absolute ETS in [15,16].

Remark 2. From (3), one has $t_{k+1}h - t_kh \geq h > 0, k \in \mathbb{N}$, which means that there is no Zeno behavior under the proposed PTS. In engineering applications, a logic "AND" gate can be used to implement PTS (3).

At triggered time t_kh, the system output $y(t_kh)$ is transmitted to the controller via the network and suffers transmission delay τ_{t_k}. Assume that $\tau_{t_0} = 0$ and $\bar{\tau} = \sup_{t_k\in\mathbb{N}}\{\tau_{t_k}\}$. Thus, the time sequence of the controller receiving the system output information is $\{t_0h + \tau_{t_0}, t_1h + \tau_{t_1}, t_2h + \tau_{t_2}, \dots\}$.

A zero-order holder (ZOH) is introduced with the holding time interval $\Omega_k \triangleq [t_kh + \tau_{t_k}, t_{k+1}h + \tau_{t_{k+1}})$. Then the output feedback controller is

$$u(t) = Ky(t_kh), \quad t \in \Omega_k, \tag{4}$$

where K is the controller gain to be designed.

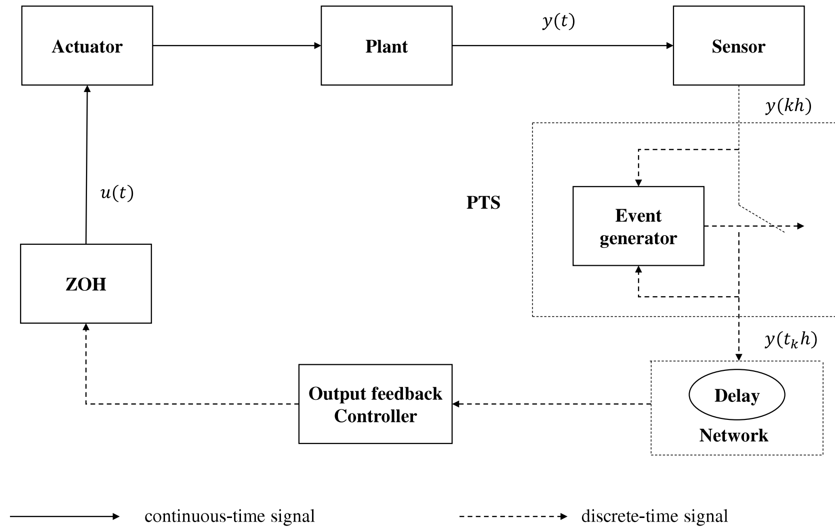

Fig. 1. Framework of a parallel-triggered NCS.

Similar with the method in [13], the holding time interval Ω_k is divided into subsets: $\Omega_k = \bigcup_{l=0}^{t_{k+1}-t_k-1} \Omega_k^l$, where $\Omega_k^l = [i_k h + \tau_{i_k}, (i_k+1)h + \tau_{i_k+1})$, $i_k h = t_k h + lh$, $l = 0, 1, \ldots, t_{k+1} - t_k - 1$. Define $\tau_{i_k+1} = \tau_{t_k}$ for $l = 0, 1, \ldots, t_{k+1}-t_k-2$ and $\tau_{i_k+1} = \tau_{t_{k+1}}$ for $l = t_{k+1} - t_k - 1$. Denote $\tau(t) \triangleq t - i_k h$ and $e(i_k h) \triangleq y(t_k h) - y(i_k h)$ for $t \in \Omega_k^l$. Note that $0 \le \tau(t) \le h + \bar{\tau} \triangleq \tau_m$. Therefore, the closed-loop system is

$$\dot{x}(t) = Ax(t) + BKCx(t - \tau(t)) + BKe(i_k h), \quad t \in \Omega_k^l, \tag{5}$$

where the initial state is $x(t) = \varphi(t)$, $t \in [-\tau_m, 0]$, $\varphi(t_0) = x_0$ and $\varphi(t)$ is continuous on $[-\tau_m, 0]$.

The goal of this paper is to design the output feedback controller (4) such that system (5) is globally asymptotically stable under the proposed PTS (3). To this end, some technical lemmas are presented as follows.

Lemma 1 ([24]). *Given a matrix $W > 0$, for any continuously differentiable function ω in $[a, b] \mapsto \mathbb{R}^m$, the following inequality holds:*

$$\int_a^b \dot{\omega}^T(s) W \dot{\omega}(s) ds \ge \frac{1}{b-a} (\omega(b) - \omega(a))^T W (\omega(b) - \omega(a)) + \frac{3}{b-a} \upsilon^T W \upsilon, \tag{6}$$

where $\upsilon = \omega(b) + \omega(a) - \frac{2}{b-a} \int_a^b \omega(s) ds$.

Lemma 2 ([25]). *Given scalars $m, n \in \mathbb{N}_{>0}$, $\mu \in (0, 1)$, matrices M_1, $M_2 \in \mathbb{R}^{n \times m}$ and positive definite matrix $R \in \mathbb{R}^{n \times n}$, for any vector $\phi \in \mathbb{R}^m$, define the function $\Xi(\mu, R)$ as:*

$$\Xi(\mu, R) = \frac{1}{\mu} \phi^T M_1^T R M_1 \phi + \frac{1}{1-\mu} \phi^T M_2^T R M_2 \phi. \tag{7}$$

If there exists a matrix $X \in \mathbb{R}^{n \times n}$ such that $\begin{bmatrix} R & X \\ X^T & R \end{bmatrix} > 0$, then the following inequality holds:

$$\min_{\mu \in (0,1)} \Xi(\mu, R) \ge \begin{bmatrix} M_1 \phi \\ M_2 \phi \end{bmatrix}^T \begin{bmatrix} R & X \\ X^T & R \end{bmatrix} \begin{bmatrix} M_1 \phi \\ M_2 \phi \end{bmatrix}. \tag{8}$$

Lemma 3. *The following two statements are equivalent:*

(i) There exist matrices $P > 0$ and $X \ge 0$ satisfying

$$-P + A^T X A < 0, \tag{9}$$

(ii) There exist matrices $P > 0$, $X \ge 0$ and a matrix Y satisfying

$$\begin{bmatrix} -P & (YA)^T \\ YA & -Y - Y^T + X \end{bmatrix} < 0. \tag{10}$$

Proof. Firstly, because inequality (9) is a strict inequality, statement (i) is equivalent to

(iii) There exist matrices $P > 0$, $X \ge 0$ and a sufficiently small positive number a satisfying

$$-P + A^T (X + aI) A < 0. \tag{11}$$

Then, similar to the proof of Theorem 1 in [26], statement (iii) holds if and only if

(iv) There exist matrices $P > 0$, $X \ge 0$, a matrix Y and a sufficiently small positive number a satisfying

$$\begin{bmatrix} -P & (YA)^T \\ YA & -Y - Y^T + X + aI \end{bmatrix} < 0. \tag{12}$$

Next, because inequality (12) is also a strict inequality, statement (iv) is equivalent to statement (ii). Thus, statements (i) and (ii) are equivalent. The proof is completed. □

Remark 3. Lemma 3 is an extension of Theorem 1 in [26]. If let $P = X > 0$, then Lemma 3 is reduced to Theorem 1 in [26].

3. Parallel-triggered control

In this section, sufficient conditions are firstly established for the closed-loop system (5) to be globally asymptotically stable. Then, sufficient conditions are derived for the output feedback controller design.

3.1. Stability analysis

Theorem 1. *Consider the closed-loop system (5) under PTS (3). For given δ, τ_m, σ and K, if there exist $n \times n$ matrices $P > 0$, $Q > 0$, $S > 0$, $R > 0$, $X_i (i = 1, 2, 3, 4)$, and a $p \times p$ matrix $\Phi > 0$ such that*

$$\Psi > 0, \tag{13}$$

$$\begin{bmatrix} \Pi & \Upsilon^T \\ \Upsilon & -R \end{bmatrix} < 0, \tag{14}$$

where

$$\Psi = \begin{bmatrix} R & 0 & X_1 & X_2 \\ \star & 3R & X_3 & X_4 \\ \star & \star & R & 0 \\ \star & \star & \star & 3R \end{bmatrix},$$

$$\Pi = \begin{bmatrix} \Pi_{11} & \Pi_{12} & 6\varphi R & \Pi_{14} & \Pi_{15} & PBK \\ \star & -12\varphi R & -4\varphi X_4 & 6\varphi R & \Pi_{25} & 0 \\ \star & \star & -12\varphi R & 2\varphi(-X_2^T+X_4^T) & \Pi_{35} & 0 \\ \star & \star & \star & -\varphi(4R+Q) & \Pi_{45} & 0 \\ \star & \star & \star & \star & \Pi_{55} & 0 \\ \star & \star & \star & \star & \star & -\Phi \end{bmatrix},$$

$$\varphi = e^{-\sigma\tau_m}, \quad \Pi_{11} = \mathrm{He}(PA) + Q + S - 4\varphi R + \sigma P,$$
$$\Pi_{12} = 2\varphi(X_3^T + X_4^T), \quad \Pi_{14} = \varphi(X_1^T + X_2^T - X_3^T - X_4^T),$$
$$\Pi_{15} = -\varphi(X_1^T + X_2^T + X_3^T + X_4^T + 2R) + PBKC,$$
$$\Pi_{25} = \varphi(6R - 2X_3 + 2X_4), \quad \Pi_{35} = \varphi(6R + 2X_2^T + 2X_4^T),$$
$$\Pi_{45} = -\varphi(2R + X_1 - X_2 - X_3 + X_4),$$
$$\Pi_{55} = -\varphi\left[8R + S + \mathrm{He}(-X_1 + X_2 - X_3 + X_4)\right] + \delta C^T\Phi C,$$
$$\Upsilon = \begin{bmatrix} \tau_m RA & 0 & 0 & 0 & \tau_m RBKC & \tau_m RBK \end{bmatrix},$$

then the closed-loop system (5) is globally asymptotically stable.

Proof. Choose a Lyapunov candidate function as

$$V(t) = x^T(t)Px(t) + \tau_m \int_{t-\tau_m}^{t}\int_{\nu}^{t} e^{\sigma(s-t)}\dot{x}^T(s)R\dot{x}(s)dsd\nu + \int_{t-\tau_m}^{t} e^{\sigma(s-t)}x^T(s)Qx(s)ds + \int_{t-\tau(t)}^{t} e^{\sigma(s-t)}x^T(s)Sx(s)ds, \quad t \in \Omega_k^l. \tag{15}$$

For $t \in \Omega_k^l$, the error $e(i_kh)$ caused by PTS (3) satisfies

$$e^T(i_kh)\Phi e(i_kh) < \max\{\delta y^T(i_kh)\Phi y(i_kh), \gamma(i_kh)\}. \tag{16}$$

According to PTS (3), system (5) stays either in the relative ETS or in the absolute ETS. Thus, the proof is divided into two cases.

Case 1: $\gamma(i_kh) \le \delta y^T(i_kh)\Phi y(i_kh)$. In this case, system (5) stays in the relative ETS, and we have

$$e^T(i_kh)\Phi e(i_kh) < \delta y^T(i_kh)\Phi y(i_kh) = \delta x^T(t-\tau(t))C^T\Phi Cx(t-\tau(t)). \tag{17}$$

The time derivative of $V(t)$ is

$$\begin{aligned}\dot{V}(t) = & -\sigma V(t) + \sigma x^T(t)Px(t) + 2x^T(t)P\dot{x}(t) \\ & + x^T(t)Qx(t) + x^T(t)Sx(t) \\ & + \tau_m^2\dot{x}^T(t)R\dot{x}(t) - \tau_m\int_{t-\tau_m}^{t} e^{\sigma(s-t)}\dot{x}^T(s)R\dot{x}(s)ds \\ & - e^{-\sigma\tau_m}x^T(t-\tau_m)Qx(t-\tau_m) \\ & - e^{-\sigma\tau(t)}x^T(t-\tau(t))Sx(t-\tau(t)) \\ & + e^T(i_kh)\Phi e(i_kh) - e^T(i_kh)\Phi e(i_kh).\end{aligned} \tag{18}$$

It follows from (17) and (18) that

$$\begin{aligned}\dot{V}(t) + \sigma V(t) \le & \ \sigma x^T(t)Px(t) + 2x^T(t)P\dot{x}(t) \\ & + x^T(t)Qx(t) + x^T(t)Sx(t) \\ & + \tau_m^2\dot{x}^T(t)R\dot{x}(t) - \tau_m e^{-\sigma\tau_m}\int_{t-\tau_m}^{t}\dot{x}^T(s)R\dot{x}(s)ds \\ & - e^{-\sigma\tau_m}x^T(t-\tau_m)Qx(t-\tau_m) \\ & - e^{-\sigma\tau_m}x^T(t-\tau(t))Sx(t-\tau(t)) \\ & + \delta x^T(t-\tau(t))C^T\Phi Cx(t-\tau(t)) \\ & - e^T(i_kh)\Phi e(i_kh).\end{aligned} \tag{19}$$

According to Lemma 1, we have

$$\begin{aligned}& -\tau_m e^{-\sigma\tau_m}\int_{t-\tau_m}^{t}\dot{x}^T(s)R\dot{x}(s)ds \\ & \le -e^{-\sigma\tau_m}\frac{\tau_m}{\tau_m-\tau(t)}\chi^T(t)\begin{bmatrix} e_1^T & e_2^T\end{bmatrix}\begin{bmatrix} R & 0 \\ 0 & 3R\end{bmatrix}\begin{bmatrix} e_1 \\ e_2\end{bmatrix}\chi(t) \\ & \quad - e^{-\sigma\tau_m}\frac{\tau_m}{\tau(t)}\chi^T(t)\begin{bmatrix} e_3^T & e_4^T\end{bmatrix}\begin{bmatrix} R & 0 \\ 0 & 3R\end{bmatrix}\begin{bmatrix} e_3 \\ e_4\end{bmatrix}\chi(t),\end{aligned} \tag{20}$$

where

$$\chi^T(t) = \begin{bmatrix} x^T(t) & \frac{\int_{t-\tau_m}^{t-\tau(t)}x^T(s)ds}{\tau_m-\tau(t)} & \frac{\int_{t-\tau(t)}^{t}x^T(s)ds}{\tau(t)} & x^T(t-\tau_m) & x^T(t-\tau(t))\end{bmatrix},$$
$$e_1 = \begin{bmatrix} 0 & 0 & 0 & -I_n & I_n\end{bmatrix}, \quad e_2 = \begin{bmatrix} 0 & -2I_n & 0 & I_n & I_n\end{bmatrix},$$
$$e_3 = \begin{bmatrix} I_n & 0 & 0 & 0 & -I_n\end{bmatrix}, \quad e_4 = \begin{bmatrix} I_n & 0 & -2I_n & 0 & I_n\end{bmatrix}.$$

Notice that (13) holds, it follows from Lemma 2 that

$$-\tau_m e^{-\sigma\tau_m}\int_{t-\tau_m}^{t}\dot{x}^T(s)R\dot{x}(s)ds \le -e^{-\sigma\tau_m}\chi^T(t)\Gamma^T\Psi\Gamma\chi(t), \tag{21}$$

where $\Gamma^T = \begin{bmatrix} e_1^T & e_2^T & e_3^T & e_4^T\end{bmatrix}$, and Ψ is given in (13).

Substituting (21) into (19) gives

$$\dot{V}(t) + \sigma V(t) \le \xi^T(t)\left[\Pi + \Upsilon^T R^{-1}\Upsilon\right]\xi(t), \tag{22}$$

where $\xi^T(t) = \begin{bmatrix} \chi^T(t) & e^T(i_kh)\end{bmatrix}$, and Υ and Π are given in (14).

Applying Schur complement, inequality (14) is equivalent to

$$\Pi + \Upsilon^T R^{-1}\Upsilon < 0. \tag{23}$$

Therefore, we have

$$\dot{V}(t) < -\sigma V(t), \quad t \in \Omega_k^l. \tag{24}$$

Case 2: $\gamma(i_kh) > \delta y^T(i_kh)\Phi y(i_kh)$. In this case, system (5) stays in the absolute ETS, and we have

$$e^T(i_kh)\Phi e(i_kh) < \gamma(i_kh) = \gamma(t-\tau(t)). \tag{25}$$

Replacing inequality (17) by inequality (25), and adopting the similar derivation in Case 1, we obtain

$$\begin{bmatrix} \bar{\Pi} & \Upsilon^T \\ \Upsilon & -R\end{bmatrix} \le \begin{bmatrix} \Pi & \Upsilon^T \\ \Upsilon & -R\end{bmatrix} < 0, \tag{26}$$

where $\bar{\Pi} = \Pi|_{\delta=0}$.

Therefore, we have

$$\begin{aligned}\dot{V}(t) & \le -\sigma V(t) + \gamma(t-\tau(t)) \\ & \le -\sigma V(t) + \gamma(t-\tau_m), \quad t \in \Omega_k^l.\end{aligned} \tag{27}$$

In view of (24) in Case 1 and (27) in Case 2, we have

$$\begin{aligned}\dot{V}(t) & \le \max\{-\sigma V(t), -\sigma V(t) + \gamma(t-\tau_m)\} \\ & = -\sigma V(t) + \gamma(t-\tau_m), \quad t \in \Omega_k^l.\end{aligned} \tag{28}$$

Integrating (28) from T_{i_k} to t, we have

$$\begin{aligned}V(t) & \le e^{-\sigma(t-T_{i_k})}V(T_{i_k}) + \int_{T_{i_k}}^{t} e^{-\sigma(t-s)}\gamma(s-\tau_m)ds \\ & = e^{-\sigma(t-T_{i_k})}V(T_{i_k}) + c_1e^{-\sigma t}\int_{T_{i_k}}^{t} e^{(\sigma-\alpha\ln\varepsilon)s}ds,\end{aligned} \tag{29}$$

where $c_1 = c\varepsilon^{\alpha\tau_m}$ and $T_{i_k} = i_kh + \tau_{i_k}$.

Notice that a Lyapunov function is used in the two cases, and $\gamma(t)$ is continuous for all $t \ge 0$. Using the comparison lemma in [27], we have

$$\begin{aligned}V(t) & \le e^{-\sigma t}V(0) + \int_0^t e^{-\sigma(t-s)}\gamma(s-\tau_m)ds \\ & = e^{-\sigma t}V(0) + c_1e^{-\sigma t}\int_0^t e^{(\sigma-\alpha\ln\varepsilon)s}ds.\end{aligned} \tag{30}$$

The following two situations are considered.

(1) If $\sigma - \alpha \ln \varepsilon = 0$, then inequality (30) becomes

$$V(t) \leq e^{-\sigma t}[V(0) + c_1 t]. \tag{31}$$

(2) If $\sigma - \alpha \ln \varepsilon \neq 0$, then inequality (30) becomes

$$V(t) \leq e^{-\sigma t}\left[V(0) - \frac{c_1}{\sigma - \alpha \ln \varepsilon}\right] + \frac{c_1 \varepsilon^{-\alpha t}}{\sigma - \alpha \ln \varepsilon}. \tag{32}$$

Therefore, for any $\sigma - \alpha \ln \varepsilon$, $\lim_{t\to+\infty} V(t) = 0$. As a result, the closed-loop system (5) is globally asymptotically stable. The proof is completed. □

Remark 4. Compared with the Lyapunov functions in [10,13], the term $e^{\sigma(s-t)}$ is introduced in this paper. This additional term plays an essential role in deriving the condition $\lim_{t\to+\infty} V(t) = 0$. Compared with the Lyapunov functions in [15,16], the double-integral term $\tau_m \int_{t-\tau_m}^{t} \int_{v}^{t} e^{\sigma(s-t)} \dot{x}^T(s) R \dot{x}(s) ds dv$ is added to our Lyapunov function. This double-integral term reduces the conservatism of the results.

Remark 5. The Wirtinger-based integral inequality is utilized in this paper to reduce the conservatism of the results, whereas Jensen's inequality is used in [16]. The Wirtinger-based integral inequality and the reciprocally convex method are utilized in this paper to reduce the computation complexity, whereas the free weighting matrix approach is used in [10,15].

Remark 6. From Theorem 1, the stability of the closed-loop system (5) is related to the parameters δ and Φ of the first parallel-triggered condition in (2), and is independent of the parameters c, ε and α of the second parallel-triggered condition in (2). However, all these parameters affect the number of transmitted signals and hence can be designed to reduce transmission rate (see Algorithm 1).

3.2. Controller design

Based on Theorem 1, now we design an output feedback controller under the proposed PTS (3).

Theorem 2. *Consider the closed-loop system (5) under PTS (3). For given δ, τ_m and σ, if there exist $n \times n$ matrices $P > 0$, $Q > 0$, $S > 0$, $R > 0$, $X_i (i = 1, 2, 3, 4)$, a $5n \times 5n$ matrix $H > 0$, a $p \times p$ matrix $\Phi > 0$, an $m \times m$ matrix Y, and an $m \times p$ matrix U such that*

$$\Psi > 0, \tag{33}$$

$$\begin{bmatrix} \Lambda_{11} + H & \Lambda_{12} & 0 & 0 \\ \star & \Lambda_{22} & \Lambda_{23} & 0 \\ \star & \star & \mathrm{He}(-B^T BY) & \Lambda_{34} \\ \star & \star & \star & -H \end{bmatrix} < 0, \tag{34}$$

where

$$\Lambda_{11} = \begin{bmatrix} \Pi_{11} & \Pi_{12} & 6\varphi R & \Pi_{14} & \tau_m (RA)^T \\ \star & -12\varphi R & -4\varphi X_4 & 6\varphi R & 0 \\ \star & \star & -12\varphi R & 2\varphi(-X_2^T + X_4^T) & 0 \\ \star & \star & \star & -\varphi(4R + Q) & 0 \\ \star & \star & \star & \star & -R \end{bmatrix},$$

$$\varphi = e^{-\sigma \tau_m},$$

$$\Lambda_{12} = \begin{bmatrix} BU & \widetilde{\Pi}_{15} \\ 0 & \Pi_{25} \\ 0 & \Pi_{35} \\ 0 & \Pi_{45} \\ \tau_m BU & \tau_m BUC \end{bmatrix}, \quad \Lambda_{22} = \begin{bmatrix} -\Phi & 0 \\ 0 & \Pi_{55} \end{bmatrix},$$

$$\Lambda_{23} = \begin{bmatrix} (B^T BU)^T \\ (B^T BUC)^T \end{bmatrix},$$

$$\Lambda_{34} = \left[(PB - BY)^T \quad 0 \quad 0 \quad 0 \quad \tau_m (RB - BY)^T\right],$$

$$\widetilde{\Pi}_{15} = -\varphi(X_1^T + X_2^T + X_3^T + X_4^T + 2R) + BUC,$$

Ψ is defined in (13), and Π_{11}, Π_{12}, Π_{14}, Π_{25}, Π_{35}, Π_{45} and Π_{55} are given in (14), then the closed-loop system (5) is globally asymptotically stable with output feedback controller gain $K = Y^{-1}U$.

Proof. Applying Schur complement, inequality (34) becomes

$$\begin{bmatrix} \Lambda_{11} + H & \Lambda_{12} & 0 \\ \star & \Lambda_{22} & \Sigma^T Y^T B^T B \\ \star & \star & \mathrm{He}(-B^T BY) + \Lambda_{34} H^{-1} \Lambda_{34}^T \end{bmatrix} < 0, \tag{35}$$

where $\Sigma = \left[Y^{-1}U \quad Y^{-1}UC\right]$.

According to Lemma 3, inequality (35) is equivalent to

$$\begin{bmatrix} \Lambda_{11} + H & \Lambda_{12} \\ \star & \Lambda_{22} + \Sigma^T \Lambda_{34} H^{-1} \Lambda_{34}^T \Sigma \end{bmatrix} < 0. \tag{36}$$

Note that

$$\begin{aligned} &\mathrm{He}\left\{\begin{bmatrix} I_{5n} \\ 0_{(p+n)\times 5n} \end{bmatrix} \Lambda_{34}^T \Sigma \left[0_{(p+n)\times 5n} \quad I_{p+n}\right]\right\} \\ &\leq \begin{bmatrix} I_{5n} \\ 0_{(p+n)\times 5n} \end{bmatrix} H \left[I_{5n} \quad 0_{5n\times(p+n)}\right] \\ &\quad + \begin{bmatrix} 0_{5n\times(p+n)} \\ I_{p+n} \end{bmatrix} \Sigma^T \Lambda_{34} H^{-1} \Lambda_{34}^T \Sigma \left[0_{(p+n)\times 5n} \quad I_{p+n}\right]. \end{aligned} \tag{37}$$

Based on (36) and (37), we have

$$\begin{bmatrix} \Lambda_{11} & \Lambda_{12} \\ \star & \Lambda_{22} \end{bmatrix} + \mathrm{He}\left\{\begin{bmatrix} I_{5n} \\ 0_{(p+n)\times 5n} \end{bmatrix} \Lambda_{34}^T \Sigma \left[0_{(p+n)\times 5n} \quad I_{p+n}\right]\right\} < 0. \tag{38}$$

Then, inequality (38) can be expressed as

$$\begin{bmatrix} \Lambda_{11} & \widetilde{\Lambda}_{12} \\ \star & \Lambda_{22} \end{bmatrix} < 0, \tag{39}$$

where $\widetilde{\Lambda}_{12} = \Lambda_{12} + \Lambda_{34}^T \Sigma$.

Pre-multiply and post-multiply (39) with

$$\begin{bmatrix} I_n & 0 & 0 & 0 & 0 & 0 & 0 \\ 0 & I_n & 0 & 0 & 0 & 0 & 0 \\ 0 & 0 & I_n & 0 & 0 & 0 & 0 \\ 0 & 0 & 0 & I_n & 0 & 0 & 0 \\ 0 & 0 & 0 & 0 & 0 & 0 & I_n \\ 0 & 0 & 0 & 0 & 0 & I_p & 0 \\ 0 & 0 & 0 & 0 & I_n & 0 & 0 \end{bmatrix}$$

and its transpose, inequality (39) becomes inequality (14). Thus, condition (34) ensures condition (14) in Theorem 1 holds. Based on Theorem 1, system (5) is globally asymptotically stable. The proof is completed. □

Remark 7. For given δ, one can first obtain K and Φ by applying Theorem 2. Then the parameters c, ε and α can be tuned to reduce transmission rate (see Algorithm 2).

Remark 8. Similar sufficient conditions have been derived for the output feedback controller design in [13]. The differences are as follows: (1) Lemma 3 is used in this paper, whereas Theorem 1 in [26] is used in [13]. From Remark 3, Theorem 1 in [26] is not applicable to our results. (2) The relative ETS is used in [13], whereas the proposed PTS (3) is utilized in this paper. Moreover, the present sampled output $y(j_k h)$ is utilized in the relative threshold function $\delta y^T(j_k h)\Phi y(j_k h)$ in this paper. In [13], the latest triggered output $y(t_k h)$ is used in the relative threshold function $\delta y^T(t_k h)\Phi y(t_k h)$.

Remark 9. Using LMIs is better than using Lyapunov equality in this paper. The reasons are as follows: (1) If using Lyapunov equality, the Lyapunov equality will contain the integral term $-\tau_m \int_{t-\tau_m}^{t} e^{\sigma(s-t)}\dot{x}^T(s)R\dot{x}(s)ds$. As a result, the Lyapunov equality is hard to be solved. Besides, the matrices of Lyapunov equality are required to be given in advance. (2) If using LMIs, this integral term can be magnified by applying Lemmas 1 and 2. Moreover, solving inequalities is generally easier than solving equalities.

3.3. Analysis of the minimum inter-event interval

The main character of PTS (3) is the potential reduction of the number of transmitted signals, which are analyzed in the following theorem.

Theorem 3. *Consider the closed-loop system (5). The lower bound on the minimum inter-event interval under PTS (3) is not smaller than the ones obtained in [9,10,15,16].*

Proof. Firstly, we derive that $t_{k+1}^{\text{PTS}}h \geq t_{k+1}^{\text{AETS}}h$ holds for a given state $x(t_k h)$, where $t_{k+1}^{\text{PTS}}h$ and $t_{k+1}^{\text{AETS}}h$ denote the next triggered time instant judged by PTS (3) and the absolute ETSs in [15,16], respectively. On the contrary, assume that $t_{k+1}^{\text{PTS}}h < t_{k+1}^{\text{AETS}}h$. Then according to the event-triggered conditions in [15,16], we obtain

$$e^T(t_{k+1}^{\text{PTS}}h)\Phi e(t_{k+1}^{\text{PTS}}h) < \gamma(t_{k+1}^{\text{PTS}}h). \tag{40}$$

Moreover, noticing (3), we have

$$e^T(t_{k+1}^{\text{PTS}}h)\Phi e(t_{k+1}^{\text{PTS}}h) \geq \max\{\delta y^T(t_{k+1}^{\text{PTS}}h)\Phi y(t_{k+1}^{\text{PTS}}h), \gamma(t_{k+1}^{\text{PTS}}h)\}, \tag{41}$$

which contradicts (40). Therefore, we can draw that $t_{k+1}^{\text{PTS}}h \geq t_{k+1}^{\text{AETS}}h$, i.e. $t_{k+1}^{\text{PTS}}h - t_k h \geq t_{k+1}^{\text{AETS}}h - t_k h$.

Similar with the above proof, we can derive that $t_{k+1}^{\text{PTS}}h \geq t_{k+1}^{\text{RETS}}h$ holds for a given state $x(t_k h)$, where $t_{k+1}^{\text{RETS}}h$ denotes the next triggered time instant determined by the relative ETSs in [9,10]. This completes the proof. □

Remark 10. The obtained lower bound of the inter-event interval is not smaller than those in [9,10,15,16]. Enlarging the minimum inter-event interval is helpful to reduce the number of transmitted signals. The advantage is shown in the examples.

4. Numerical algorithms

In this section, an algorithm is proposed to design the optimal parameters of PTS (3) for the given controller. Similar to this algorithm, a co-design algorithm is developed to obtain both the optimal trigger parameters and the controller gain in the sense that the transmission rate is minimized.

4.1. Design of the optimal trigger parameters

From Remark 6, the parameters δ and Φ of PTS (3) achieved by Theorem 1 are only feasible solutions, and the parameters c, ε and α of PTS (3) cannot be calculated by Theorem 1. Therefore, it is necessary to propose an algorithm to obtain the optimal trigger parameters δ^*, Φ^*, c^*, ε^* and α^* to minimize transmission rate.

For this purpose, we choose the transmission rate [21]

$$r = \frac{N_T}{N_S} \tag{42}$$

as an index, where N_T and N_S are the numbers of transmitted signals and sampled signals, respectively. Based on Theorem 1, the following minimization problem is formulated:

$$\begin{cases} \min r \\ \text{subject to: (13) and (14).} \end{cases} \tag{43}$$

It is noted that $\gamma(t) = c\varepsilon^{-\alpha t} = ce^{-(\ln\varepsilon)\alpha t} = ce^{-\bar{\alpha}t}$, where $\bar{\alpha} = (\ln\varepsilon)\alpha$. Therefore, we search for the optimal value $\bar{\alpha}^*$ instead of ε^* and α^* to reduce the computation complexity. After $\bar{\alpha}^*$ is found, the optimal values of ε and α can be chosen as $\varepsilon^* = e$ and $\alpha^* = \bar{\alpha}^*$. Therefore, the proposed numerical algorithm sets $\varepsilon^* = e$ and searches for α^* directly.

Now the following numerical algorithm is given to obtain the optimal solution to problem (43).

Algorithm 1 Design of the optimal trigger parameters δ^*, Φ^*, c^*, ε^* and α^*

Step 1: Given scalars τ_m, σ, controller gain K, sampling period h and initial state x_0. Set sufficiently small scalar α_0, sufficiently large scalars $c_{\max}$, $\alpha_{\max}$, sufficiently small step increments Δ_δ, Δ_c, Δ_α and terminal time of the simulation T_f. Set $\varepsilon^* = \varepsilon = e$. Initialize $r^* = 1$.

Step 2: Obtain the optimal parameters δ^*, Φ^*, c^* and α^* as follows:

```
for δ = 0 : Δ_δ : 1 do
  Obtain Φ by solving LMIs (13) and (14) in Theorem 1.
  if Feasible Φ is found then
    for c = 0 : Δ_c : c_max do
      for α = α_0 : Δ_α : α_max do
        Calculate r during t ∈ [0, T_f] via numerical simulations.
        if r < r* then
          Update r* = r, δ* = δ, Φ* = Φ, c* = c and α* = α.
        else
          Keep r*, δ*, Φ*, c* and α*.
        end if
      end for
    end for
  else
    Go to Step 3.
  end if
end for
```

Step 3: Output the parameters δ^*, Φ^*, c^*, ε^*, α^* and the index r^*.

Remark 11. No methods are provided in [23] to seek for the optimal trigger parameters of the PTS. The algorithm in [21] obtains the optimal trigger parameters of the relative ETS. Inspired by [21], Algorithm 1 in this paper seeks for the optimal trigger parameters of PTS (3).

4.2. Co-design of the optimal trigger parameters and the controller gain

Similar to Algorithm 1, a co-design algorithm is proposed to obtain both the optimal trigger parameters δ^*, Φ^*, c^*, ε^*, α^* and the controller gain K^*:

Algorithm 2 Co-design of the trigger parameters and the controller gain

---

Step 1: Given scalars τ_m, σ, sampling period h and initial state x_0. Set sufficiently small scalar α_0, sufficiently large scalars $c_{\max}$, $\alpha_{\max}$, sufficiently small step increments Δ_δ, Δ_c, Δ_α and terminal time of the simulation T_f. Set $\varepsilon^* = \varepsilon = e$. Initialize $r^* = 1$.

Step 2: Obtain the optimal trigger parameters δ^*, Φ^*, c^*, α^* and the controller gain K^* as follows:

for $\delta = 0 : \Delta_\delta : 1$ **do**
  Obtain K and Φ by solving LMIs (33) and (34) in Theorem 2.
  if Feasible K and Φ are found **then**
    for $c = 0 : \Delta_c : c_{\max}$ **do**
      for $\alpha = \alpha_0 : \Delta_\alpha : \alpha_{\max}$ **do**
        Calculate r during $t \in [0, T_f]$ via numerical simulations.
        if $r < r^*$ **then**
          Update $r^* = r$, $\delta^* = \delta$, $\Phi^* = \Phi$, $c^* = c$, $\alpha^* = \alpha$ and $K^* = K$.
        else
          Keep r^*, δ^*, Φ^*, c^*, α^* and K^*.
        end if
      end for
    end for
  else
    Go to Step 3.
  end if
end for

Step 3: Output the parameters δ^*, Φ^*, c^*, ε^*, α^* of PTS (3) and the controller gain K^*, and the index r^*.

Remark 12. Similar co-design methods have been used in [10,13,15–17] to obtain both the feasible trigger parameters and the controller gain. In this paper, Algorithm 2 tries to find the optimal trigger parameters and the controller gain.

5. Illustrative examples

In this section, two examples are used to show the validity of our results. One is to illustrate that the proposed PTS can further reduce the number of transmitted signals compared with the schemes in [10,17,19,28–30] for the given controller. The other is to show that the co-design method is more effective than the result in [13].

Example 1. Consider an inverted pendulum on a cart investigated in [10,19,28–30]. The state equations of the plant can be described by system (1) with the following parameters:

$$A = \begin{bmatrix} 0 & 1 & 0 & 0 \\ 0 & 0 & \frac{mg}{M} & 0 \\ 0 & 0 & 0 & 1 \\ 0 & 0 & \frac{g}{l} & 0 \end{bmatrix}, \quad B = \begin{bmatrix} 0 \\ \frac{1}{M} \\ 0 \\ -\frac{1}{Ml} \end{bmatrix}, \quad C = \begin{bmatrix} 1 & 0 & 0 & 0 \\ 0 & 1 & 0 & 0 \\ 0 & 0 & 1 & 0 \\ 0 & 0 & 0 & 1 \end{bmatrix},$$

where $m = 1$ kg denotes the mass of the pendulum bob, $M = 10$ kg is the cart mass, and $l = 0.3$ m is the length of the pendulum arm and $g = 10$ m/s^2 is the gravitational acceleration. The state $x = [\ x_1 \quad x_2 \quad x_3 \quad x_4\ ]^T$, where $x_i (i = 1, 2, 3, 4)$ are the cart's position, the cart's velocity, the pendulum bob's angle and the pendulum bob's angular velocity, respectively.

We set $K = [\ 2 \quad 12 \quad 378 \quad 210\ ]$, $\tau_{t_k} = \bar{\tau} = 0$, $h = 0.12$ s, $T_f = 30$ s, and the initial state $x_0 = [\ 0.98 \quad 0 \quad 0.2 \quad 0\ ]^T$, which are the same as those in [10]. It follows from $\tau_m = h + \bar{\tau}$ that $\tau_m = 0.12$. Let $\alpha_0 = 0.05$, $c_{\max} = \alpha_{\max} = 10$, $\Delta_\delta = 0.01$, $\Delta_c = \Delta_\alpha = 0.05$ and $\sigma = 0.2$.

By running Algorithm 1 in Matlab, the minimal transmission rate r^* is obtained as 20%, and the optimal parameters of PTS (3) are obtained as follows: $\delta^* = 0.23$, $c^* = 0.60$, $\varepsilon^* = e$, $\alpha^* = 0.25$ and

$$\Phi^* = \begin{bmatrix} 0.0002 & 0.0010 & 0.0310 & 0.0170 \\ 0.0010 & 0.0060 & 0.1838 & 0.1029 \\ 0.0310 & 0.1838 & 5.8170 & 3.2116 \\ 0.0170 & 0.1029 & 3.2116 & 1.7946 \end{bmatrix}.$$

Table 1
Average inter-event interval under different triggered schemes.

Triggered scheme	Average inter-event interval
The proposed PTS (3)	**0.6098**
The scheme in [19]	0.5769
The scheme in [10]	0.5131
The scheme in [28]	0.4816
The scheme in [29]	0.3917
The scheme in [30]	$< 10^{-5}$

Table 1 shows the average inter-event interval under our PTS (3) and the schemes in [10,19,28–30]. From Table 1, our PTS (3) provides a larger average inter-event interval than the existing triggered schemes in [10,19,28–30]. Therefore, our PTS (3) further reduces the amount of transmitted signals compared with the existing triggered schemes in [10,19,28–30]. Moreover, the ETS in [19] needs a continuous supervision of the sampled data, whereas our PTS (3) only needs a supervision of the sampled data at discrete time instants and hence avoids the extra hardware requirements.

Next, the comparison between the mixed ETSs and our PTS (3) is given. The mixed ETS proposed in [17] is implemented:

$$t_{k+1}h = t_k h + \min_{d \in \mathbb{N}_{>0}} \{dh | e^T(j_k h)\Phi e(j_k h) \geq \delta y^T(t_k h)\Phi y(t_k h) + \gamma(j_k h) \triangleq \eta_1(j_k h)\}. \quad (44)$$

By replacing $y(t_k h)$ by $y(j_k h)$, a new mixed ETS is also implemented:

$$t_{k+1}h = t_k h + \min_{d \in \mathbb{N}_{>0}} \{dh | e^T(j_k h)\Phi e(j_k h) \geq \delta y^T(j_k h)\Phi y(j_k h) + \gamma(j_k h) \triangleq \eta_2(j_k h)\}. \quad (45)$$

The parameters δ, Φ, c, ε and α are set as mentioned above. The simulation results are illustrated in Figs. 2–4. From Fig. 2, the system responses under the proposed PTS (3) are similar to that under the mixed ETS in [17] (that is, (44)) and the mixed ETS (45). According to Fig. 3, the mixed ETS in [17], the mixed ETS (45) and our PTS (3) have transmitted 73, 55 and 50 signals, respectively. Therefore, compared to the mixed ETS in [17] and the mixed ETS (45), our PTS (3) can further reduce the amount of transmitted signals while maintaining the global asymptotical stability. From Fig. 4(c), the system stays in the absolute ETS during $t \in [0, 3.24\text{ s}]$, and stays in the relative ETS during $t \in [3.24\text{ s}, 30\text{ s}]$, which verifies the advantages of using both the relative error and the absolute error information.

Fig. 5 shows the number of transmitted data under the mixed ETS in [17], the mixed ETS (45) and the proposed PTS (3) during different time periods. In the interval $[0, 2.5\text{ s}]$, 6, 6 and 7 signals have been transmitted under the mixed ETS [17], the mixed ETS (45) and the proposed PTS (3), respectively. It can be seen that the number of transmitted signals under our PTS (3) is larger than that under the mixed ETS in [17] and the mixed ETS (45). In this case, the system performance is maintained and fewer signals need to be sent during $t \in [2.5\text{ s}, 30\text{ s}]$. Therefore, the transmission rate under our PTS (3) is smallest during the whole operation, even though the triggered condition under the mixed ETS (45) is stricter than that under our PTS (3).

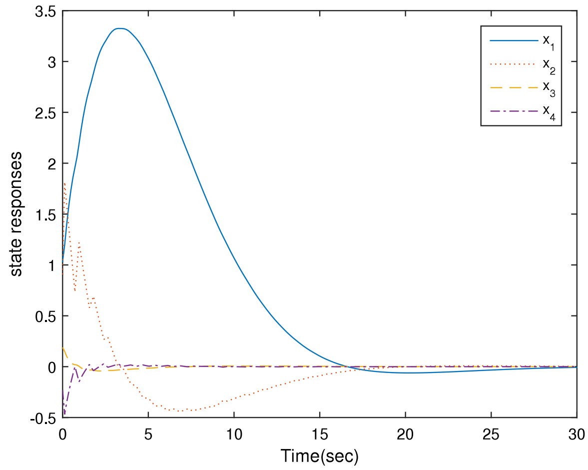

(a) System states under the ETS in [17]

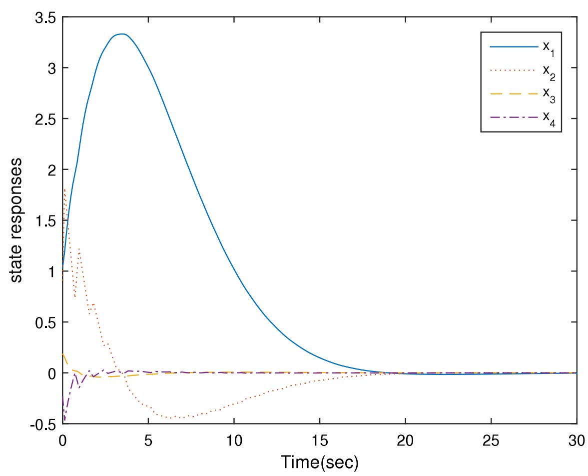

(b) System states under the ETS (45)

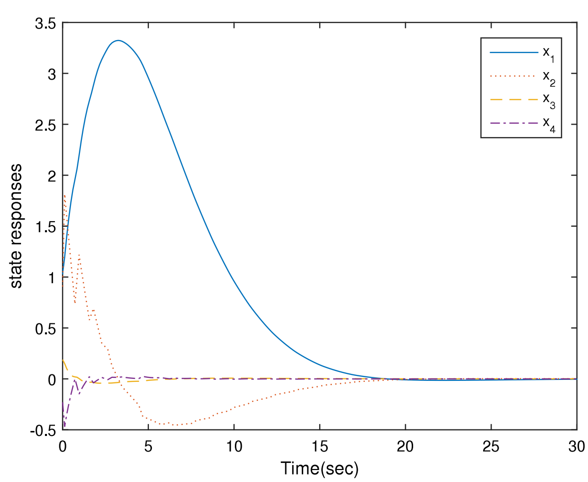

(c) System states under the proposed PTS (3)

Fig. 2. Comparison of the system states under three different triggered schemes both with $\delta = 0.23$, $c = 0.6$, $\varepsilon = e$ and $\alpha = 2.5$.

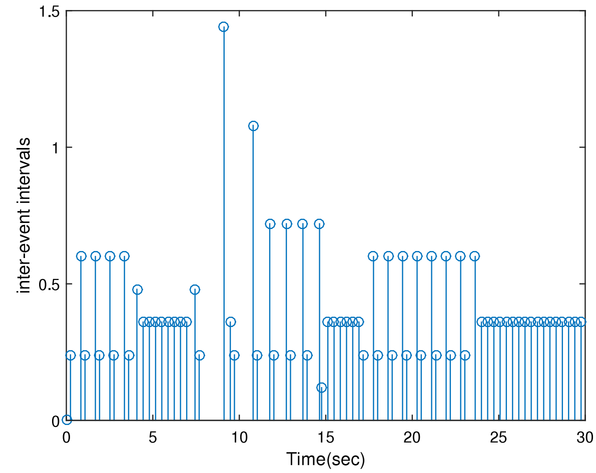

(a) Inter-event intervals under the ETS in [17]

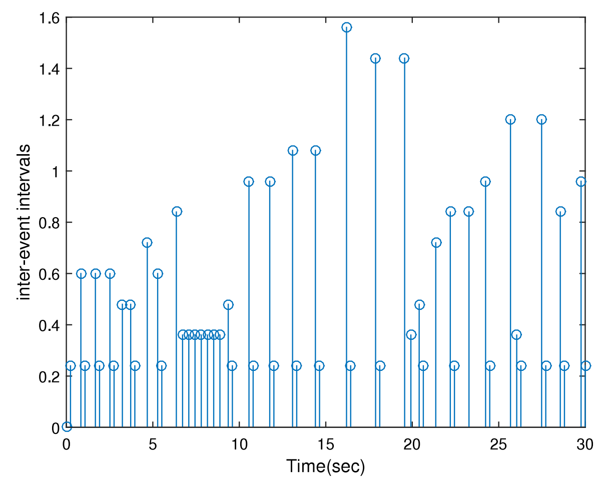

(b) Inter-event intervals under the ETS (45)

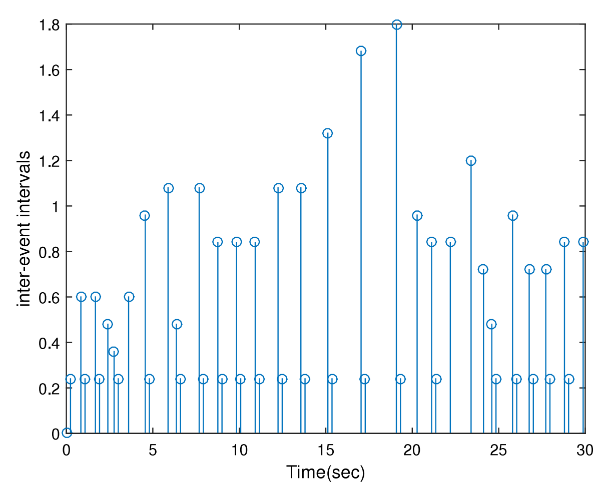

(c) Inter-event intervals under the proposed PTS (3)

Fig. 3. Comparison of the inter-event intervals under three different triggered schemes both with $\delta = 0.23$, $c = 0.6$, $\varepsilon = e$ and $\alpha = 2.5$.

Example 2. Consider system (1) with the following parameters borrowed from [13]:

$$A = \begin{bmatrix} -1 & 0.1 \\ 0.2 & 0.2 \end{bmatrix}, \quad B = \begin{bmatrix} 1 \\ 1 \end{bmatrix}, \quad C = \begin{bmatrix} 1 & 1 \end{bmatrix}.$$

We set $\tau_m = 0.5$, $h = 0.01$ s, $T_f = 30$ s, and the initial state $x_0 = [\ 3 \quad -4\ ]^T$, which are the same as those in [13]. Let $\alpha_0 = 0.05$, $c_{\max} = \alpha_{\max} = 20$, $\Delta_\delta = 0.01$, $\Delta_c = \Delta_\alpha = 0.05$ and $\sigma = 0.02$.

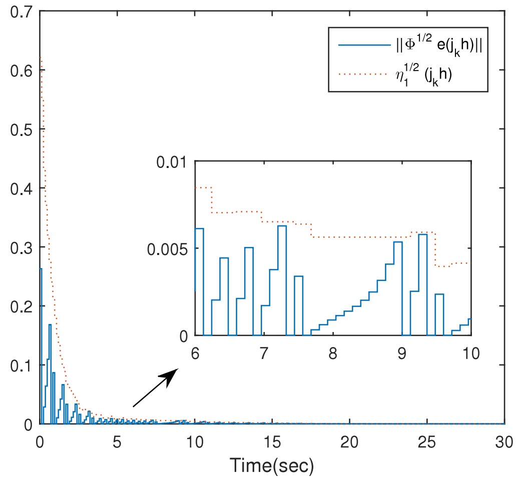

(a) Error signals under the ETS in [17]

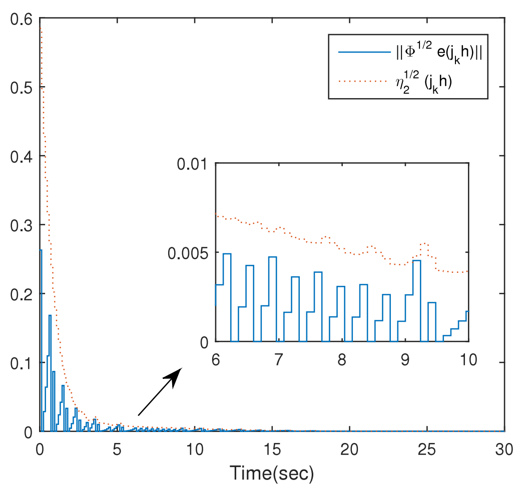

(b) Error signals under the ETS (45)

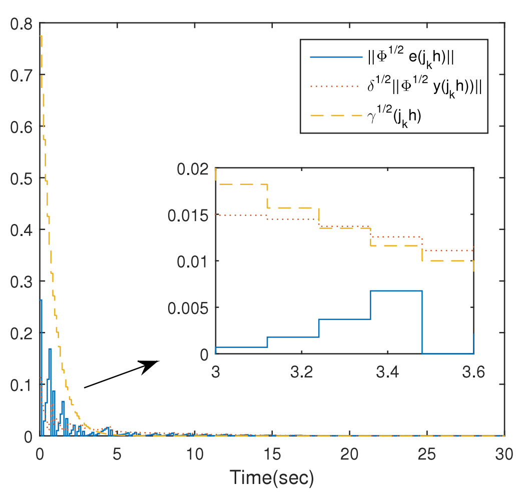

(c) Error signals under the proposed PTS (3)

Fig. 4. Comparison of the error signals under three different triggered schemes both with $\delta = 0.23$, $c = 0.6$, $\varepsilon = e$ and $\alpha = 2.5$.

To compare with the controller design method in [13], set $\tau_{t_k} = 0$. By employing Theorem 1 in [13] and Theorem 2 in this paper, the corresponding controller gains K and the weighting matrices

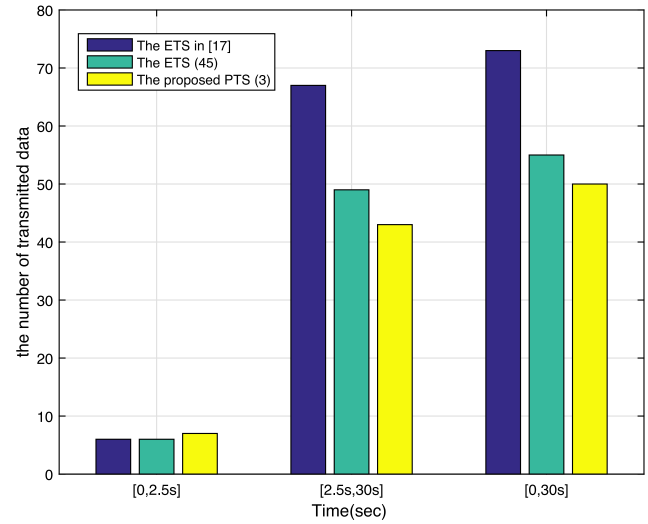

Fig. 5. Comparison of the number of transmitted data under three different triggered schemes both with $\delta = 0.23$, $c = 0.6$, $\varepsilon = e$ and $\alpha = 2.5$.

Table 2
Controller gain K and weighting matrix Φ.

δ		0.1	0.2	0.3
Theorem 1 in [13]	K	−0.4317	−0.4039	−0.3754
	Φ	3.1604	1025.9678	732.9611
Theorem 2	K	−0.4743	−0.5049	−0.5402
	Φ	3.8522	751.2036	3.1411

Φ for different δ are listed in Table 2. For the case $\delta = 0.1$ in Table 2, the controller gain $K = -0.4743$ and the weighting matrix $\Phi = 3.8522$ are obtained by using Theorem 2. From Remark 7, the other parameters of the proposed PTS (3) are obtained as follows: $c = 1$, $\varepsilon = e$ and $\alpha = 0.2$. With the above controller gains K and the weighting matrices Φ for the case $\delta = 0.1$, the simulation results are shown in Figs. 6 and 7. According to Fig. 6, the global asymptotical stability performance achieved by Theorem 2 is better than that by Theorem 1 in [13]. Hence, the controller design method in this paper is more effective than the result in [13]. Fig. 7 illustrates that the relative ETS in [13] and our PTS (3) have transmitted 19 and 14 data, respectively. Therefore, our PTS (3) reduces 26.32% signal transmission compared to the relative ETS in [13], which validates the effectiveness of the proposed PTS (3).

Next, the co-design issue is addressed. By applying Algorithm 2, the transmission rate r^* is minimized to 0.2%, the optimal parameters of the proposed PTS (3) and the controller gain are obtained as follows: $\delta^* = 0.25$, $\Phi^* = 2.5293$, $c^* = 8.35$, $\varepsilon^* = e$, $\alpha^* = 0.15$ and $K^* = -0.5239$. Note that $\tau_m = h + \bar{\tau}$, we have $\bar{\tau} = 0.49$. The transmission delay τ_{t_k} is uniformly generated on the interval [0, 0.49]. Both the delay-free and the time-delay cases are performed. The simulation results are shown in Figs. 8 and 9. From Fig. 8, the system performances are deteriorated in the two cases. Fig. 9 shows that 6 and 8 data have been transmitted in the delay-free case and the time-delay case, respectively. Therefore, a trade-off needs to be conducted between the transmission rate and the system performance. More signals need to be transmitted while the system performance needs to be maintained.

6. Conclusions

This paper studied the parallel-triggered static output stabilization problem of linear networked control systems. A new parallel-triggered scheme was proposed by using both the relative error

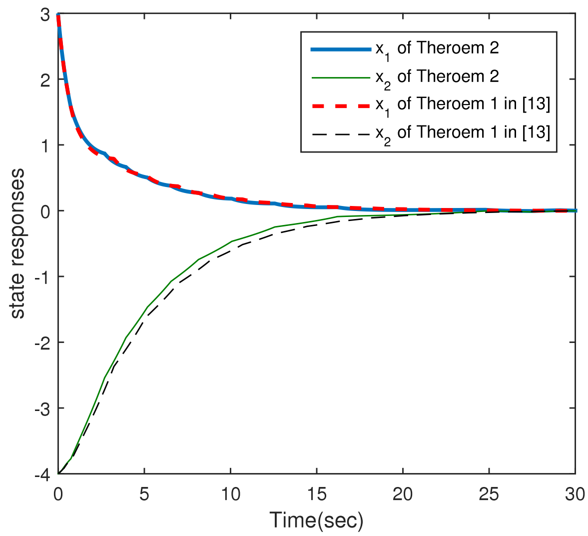

Fig. 6. Comparison of the state responses achieved by Theorem 1 in [13] and Theorem 2 in this paper.

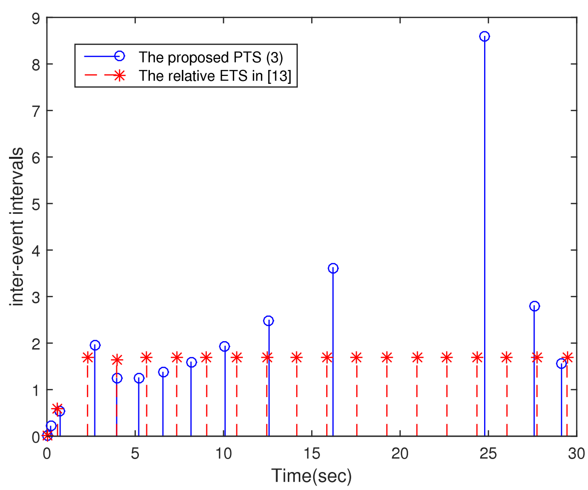

Fig. 7. Comparison of the inter-event intervals under the relative ETS in [13] and the proposed PTS (3).

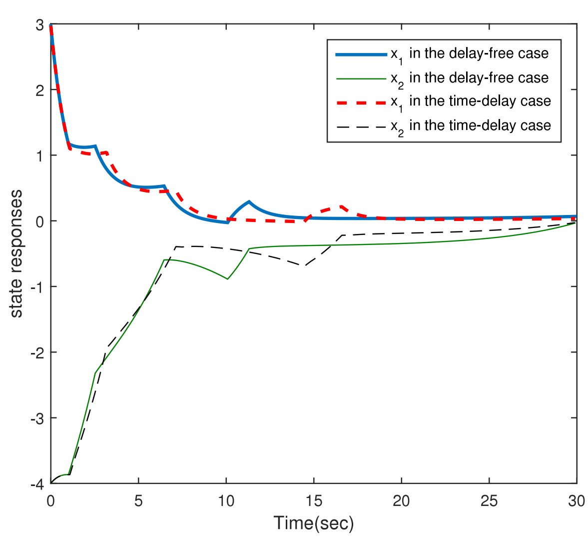

Fig. 8. State responses under the co-design algorithm.

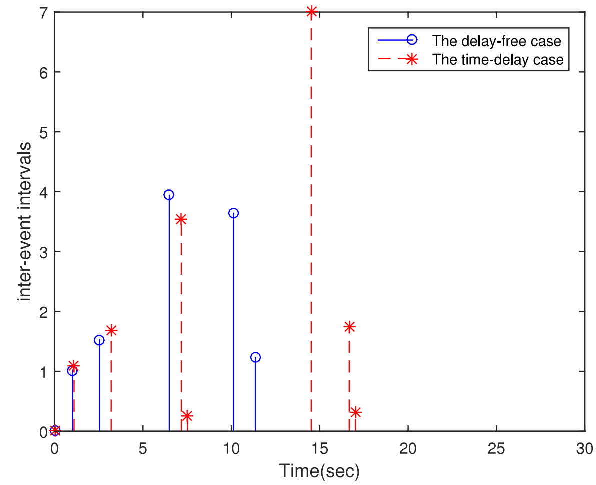

Fig. 9. Inter-event intervals under the co-design algorithm.

and the absolute error information. The linear parallel-triggered networked control system was modeled as a time-delay system. Based on the model, sufficient conditions were derived for global asymptotical stability in terms of linear matrix inequalities. A co-design algorithm was developed to obtain both the optimal trigger parameters and the output feedback controller gain. Finally, two examples were given to show the effectiveness of the proposed scheme.

The advantage of the proposed scheme is that it can reduce the number of transmitted signals while maintaining the global asymptotical stability. Moreover, the proposed parallel-triggered scheme is a generalization of the relative and the absolute event-triggered schemes. Compared with the previous methods, the co-design algorithm developed in this paper obtains both the optimal trigger parameters and the output feedback controller gain. However, the proposed co-design algorithm is a bit time-consuming according to our computations. Therefore, searching for more efficient algorithms could be a potential research direction. Moreover, this work will be extended to nonlinear control systems in the future.

References

[1] Zhang L, Gao H, Kaynak O. Network-induced constraints in networked control systems—A survey. IEEE Trans. Ind. Inf. 2013;9(1):403–16.
[2] Liu S, Liu PX, El Saddik A. Modeling and stability analysis of automatic generation control over cognitive radio networks in smart grids. IEEE Trans. Syst Man Cybern.: Syst. 2015;45(2):223–34.
[3] Gupta RA, Chow M-Y. Networked control system: overview and research trends. IEEE Trans Ind Electron 2010;57(7):2527–35.
[4] Zhang X-M, Han Q-L, Yu X. Survey on recent advances in networked control systems. IEEE Trans. Ind. Inf. 2016;12(5):1740–52.
[5] Xiong J, Lam J. Stabilization of linear systems over networks with bounded packet loss. Automatica 2007;43(1):80–7.
[6] Jiang S, Fang H. H_∞ static output feedback control for nonlinear networked control systems with time delays and packet dropouts. ISA Trans 2013;52(2):215–22.
[7] Zhang D, Shi P, Wang Q-G, Yu L. Analysis and synthesis of networked control systems: a survey of recent advances and challenges. ISA Trans 2017;66:376–92.
[8] Zhang X-M, Han Q-L, Zhang B-L. An overview and deep investigation on sampled-data-based event-triggered control and filtering for networked systems. IEEE Trans. Ind. Inf. 2017;13(1):4–16.
[9] Hu S, Yue D. Event-triggered control design of linear networked systems with quantizations. ISA Trans 2012;51(1):153–62.
[10] Yue D, Tian E, Han Q-L. A delay system method for designing event-triggered controllers of networked control systems. IEEE Trans Automat Control 2013;58(2):475–81.
[11] Tabuada P. Event-triggered real-time scheduling of stabilizing control tasks. IEEE Trans Automat Control 2007;52(9):1680–5.

[12] Mahmoud MS, Sabih M, Elshafei M. Event-triggered output feedback control for distributed networked systems. ISA Trans 2016;60:294–302.
[13] Shen M, Yan S, Zhang G. A new approach to event-triggered static output feedback control of networked control systems. ISA Trans 2016;65:468–74.
[14] Lunze J, Lehmann D. A state-feedback approach to event-based control. Automatica 2010;46(1):211–5.
[15] Zhang J, Feng G. Event-driven observer-based output feedback control for linear systems. Automatica 2014;50(7):1852–9.
[16] Yan S, Shen M, Zhang G. Extended event-driven observer-based output control of networked control systems. Nonlinear Dynam 2016;86(3):1639–48.
[17] Li F, Fu J, Du D. An improved event-triggered communication mechanism and $\mathcal{L}_\infty$ control co-design for network control systems. Inform Sci 2016;370:743–62.
[18] Donkers M, Heemels W. Output-based event-triggered control with guaranteed $\mathcal{L}_\infty$-gain and improved and decentralized event-triggering. IEEE Trans Automat Control 2012;57(6):1362–76.
[19] Selivanov A, Fridman E. Event-Triggered H_∞ Control: A switching approach. IEEE Trans Automat Control 2016;61(10):3221–6.
[20] Gu Z, Yang L, Tian E, Zhao H. Event-triggered reliable H_∞ filter design for networked systems with multiple sensor distortions: A probabilistic partition approach. ISA Trans 2017;66:2–9.
[21] Peng C, Han Q-L. A novel event-triggered transmission scheme and $\mathcal{L}_2$ control co-design for sampled-data control systems. IEEE Trans Automat Control 2013;58(10):2620–6.
[22] Borgers DN, Heemels WM. Event-separation properties of event-triggered control systems. IEEE Trans Automat Control 2014;59(10):2644–56.
[23] Sun X-M, Wang X-F, Hong Y, Xia W. Stabilization control design with parallel-triggering mechanism. IEEE Trans Ind Electron 2017;64(4):3260–7.
[24] Seuret A, Gouaisbaut F. Wirtinger-based integral inequality: application to time-delay systems. Automatica 2013;49(9):2860–6.
[25] Park P, Ko JW, Jeong C. Reciprocally convex approach to stability of systems with time-varying delays. Automatica 2011;47(1):235–8.
[26] de Oliveira MC, Bernussou J, Geromel JC. A new discrete-time robust stability condition. Systems Control Lett 1999;37(4):261–5.
[27] Khalil HK. Nonlinear Systems. 4th ed.. Prentice-Hall; 2002.
[28] Wang X. Event-triggering in cyber-physical systems (Ph.D thesis), University of Notre Dame; 2009.
[29] Wang X, Lemmon MD. Self-triggered feedback control systems with finite-gain $\mathcal{L}_2$ Stability. IEEE Trans Automat Control 2009;54(3):452–67.
[30] Tabuada P, Wang X. Preliminary results on state-triggered scheduling of stabilizing control tasks. In: 45th IEEE conference on decision and control. 2006, p. 282–7.